Carbohydrate Polymers 111 (2014) 663–669

Contents lists available at ScienceDirect

Carbohydrate Polymers

journal homepage: www.elsevier.com/locate/carbpol

Integrated biorefinery based on hydrothermal and alkaline treatments: Investigation of sorghum hemicelluloses

Shao-Long Sun, Jia-Long Wen, Ming-Guo Ma, Xian-Liang Song, Run-Cang Sun*

Beijing Key Laboratory of Lignocellulosic Chemistry, College of Material Science and Technology, Beijing Forestry University, Beijing 100083, China

ARTICLE INFO

Article history:
Received 27 January 2014
Received in revised form 19 April 2014
Accepted 25 April 2014
Available online 6 May 2014

Keywords:
Sweet sorghum stem
Hydrothermal pretreatment
Alkaline treatment
Hemicelluloses
Structural feature
Nuclear magnetic resonance (NMR)

ABSTRACT

An integrated process based on hydrothermal pretreatment (HTP) and alkaline post-treatment was proposed to treat sweet sorghum stem. The structural features of the alkali-soluble hemicelluloses (ASHs) obtained from the un-pretreated and hydrothermally pretreated materials were comprehensively investigated by HPAEC, GPC, NMR, FT-IR, and TGA techniques. The ASH with the highest yield (60.6%) was obtained from the HTP residue performed at 130 °C for 1.0 h. All the results indicated that the ASHs had a more linear structure with increasing the pretreatment temperature (110–170 °C). The molecular weights of the ASHs were decreased with increasing the pretreatment temperature, suggesting that C–O bonds in the ASHs were gradually cleaved, especially at the higher temperatures (≥170 °C). Interestingly, the integrated process yielded more homogeneous ASHs than hemicelluloses obtained from the un-pretreated material. Based on the spectral analyses, the structure of the ASHs was assumed to be L-arabino-4-*O*-methyl-D-glucurono-D-xylan.

1. Introduction

Long term economic and environmental concerns have resulted in a great amount of attention on using liquid fuels from renewable sources to replace fossil fuels in the past decades (Sun & Cheng, 2002). Lignocellulosic material has been known as one of the most promising sources of renewable energy, since it is an abundant resource, and has low CO_2 emissions and low cost (Berndes, Hoogwijk, & van den Broek, 2003; Zhao et al., 2009). Among lignocelluloses, sweet sorghum, as a potential alternative raw material for production of fuel alcohol, has drawn more and more attentions in the world (Reddy et al., 2005). This is because it is rich in cellulose, which can be used for production of biofuels, chemicals, and materials (Antonopoulou, Gavala, Skiadas, Angelopoulos, & Lyberatos, 2008; Prasad, Singh, Jain, & Joshi, 2007). However, due to the complex inherent structure of lignocelluloses, the direct enzymatic hydrolysis of cellulose is impeded. Therefore, pretreatment is a necessary step before biomass hydrolysis. The purposes of the pretreatment are listed as follows: modifying or removing lignin and/or hemicelluloses, increasing substrate surface area, disrupting cellulose crystallinity, and decreasing the degree of polymerization, which facilitates enzymes molecules accessing the rigid structure of biomass for maximum conversion of sugars (Balat, Balat, & Öz, 2008; Jørgensen, Kristensen, & Felby, 2007).

Hitherto, a variety of physical, chemical, mechanical, and biological pretreatment techniques have been reported, including the application of steam explosion (Alfani, Gallifuoco, Saporosi, Spera, & Cantarella, 2000), dilute acid (Lloyd & Wyman, 2005), hydrothermal pretreatment (HTP) (Thomsen, Thygesen, & Thomsen, 2008), and subcritical CO_2 (Zhang & Wu, 2013). Among them, HTP is an economical and eco-friendly technology for the pretreatment of lignocelluloses as compared to others, since the medium only contains feedstock and water, avoiding corrosion and acid recycling (Liu, 2010). More importantly, HTP can also achieve some important bio-products, such as hemicelluloses, oligosaccharides, and some other chemicals (e.g., furfural, formic acid, acetic acid, and levulinic acid) (Garrote, Dominguez, & Parajó, 1999; Kabel et al., 2002). However, HTP has some limitations, such as only partial removal of hemicelluloses and incomplete disruption of lignin–hemicelluloses matrix. Alkaline (sodium hydroxide) treatment is a potential technology for the removal of hemicelluloses and lignin effectively (Gabrielii, Gatenholm, Glasser, Jain, & Kenne, 2000). It is well known that hemicelluloses, as an inhomogeneous group of polysaccharides, play an important role in the restriction of cellulose accessibility (Leu & Zhu, 2012). In the biorefinery process, there is a growing interest in hemicelluloses, the second most abundant polysaccharide in lignocelluloses, for developing bio-based materials and chemicals (Sun, 2009). Hence, it is necessary to recovery the hemicelluloses, and understand the structural features

* Corresponding author. Tel.: +86 1062336903; fax: +86 1062336903.
E-mail address: rcsun3@bjfu.edu.cn (R.-C. Sun).

http://dx.doi.org/10.1016/j.carbpol.2014.04.099
0144-8617/

of hemicelluloses from the pretreated lignocelluloses, which will enhance biorefinery viability by a variety of measuring technologies in the future.

In the present study, the integrated process based on hydrothermal pretreatment (110–230 °C, 0.5–2.0 h) and sodium hydroxide post-treatment (2% NaOH) was proposed to treat sweet sorghum stem (SSS). The chemical compositions of the obtained alkali-soluble hemicelluloses (ASHs) were analyzed by high performance anion exchange chromatography (HPAEC). The molecular weights of the ASHs were determined by gel permeation chromatography (GPC). The structural features of the ASHs were extensively investigated and evaluated by nuclear magnetic resonance (NMR) and Fourier transform infrared (FT-IR) spectroscopy techniques. Moreover, to reveal the relationship between structural features and thermal behaviors of the ASHs, thermogravimetric analysis (TGA) was also applied. The well-established structure information of the ASHs will contribute to their potential use in future biorefinery industry.

2. Experimental

2.1. Materials

The raw material used in the experiment was SSS obtained from the experimental farm of the North-Western University of Agricultural and Forest Sciences and Technology (Yangling, PR China). The SSS was first dried in an oven at 60 °C for 24 h and then ground in a mill to obtain a 20–60 mesh fraction. Then the particle was treated with toluene/ethanol (2:1, v/v) in a Soxhlet apparatus for 6 h to remove extractives. The dewaxed material was subsequently extracted with hot water at 80 °C for 2 h to remove starch. The extractive-free material was dried in an oven at 60 °C for 24 and stored for use. The composition (%, w/w) of the extractive-free material was 41.1% cellulose, 28.9% hemicelluloses, and 19.5% Klason lignin, which was determined by a standard method of National Renewable Energy Laboratory's (NREL) (Sluiter et al., 2011). All experiments were analyzed in duplicate under the same conditions.

2.2. Hydrothermal pretreatment (HTP)

The HTP process was carried out in a 1000 mL stainless steel autoclave (Parr, USA) with a magnetic stirrer at a solid to liquor ratio of 1:10 (g/mL) by a PID controller (Parr 4848, USA). The HTP experiments were divided into nine batches, in each batch, 15 g the extractive-free material was mixed with 150 mL deionized water. Then the mixture was heated at 110, 130 or 150 °C for 1.0 h, 170 °C for different periods (0.5, 1.0 or 2.0 h), or 190, 210 or 230 °C for 0.5 h. After HTP, the mixtures were cooled to room temperature and then filtrated with a Buchner funnel. The obtained solid residues were washed repeatedly with distilled water until the filtrates were neutral (pH 7.0). Then the solids were dried in a cabinet oven at 60 °C for 16 h.

2.3. Fractionation of alkali-soluble hemicelluloses (ASHs)

The isolation procedure for the ASHs from the un-pretreated and hydrothermally pretreated material (the extractive-free) is shown in Fig. 1. HTP residue (5 g) was treated with 2% NaOH aqueous solution at 90 °C for 2 h under a solid to liquid ratio of 1:20 (g/mL). The liquid fractions were collected, neutralized to pH 5.5–6.0 with 6 M HCl, and further concentrated to 20–30 mL with a rotary evaporator under reduced pressure. Subsequently, the concentrated solutions were poured into three volumes of 95% ethanol with vigorous stirring, and hemicelluloses were recovered by filtering and freeze-drying. The obtained ASHs were labeled as $H_{110(1.0)}$, $H_{130(1.0)}$, $H_{150(1.0)}$, $H_{170(0.5)}$, $H_{170(1.0)}$, $H_{170(2.0)}$, $H_{190(0.5)}$, $H_{210(0.5)}$, and $H_{230(0.5)}$, corresponding to the pretreatment conditions at 110, 130, and 150 °C for 1 h, 170 °C for different periods (0.5, 1.0, and 2.0 h), and 190, 210, and 230 °C for 0.5 h, respectively. Control hemicelluloses extracted from the un-pretreated material was labeled as HR under the same alkaline condition.

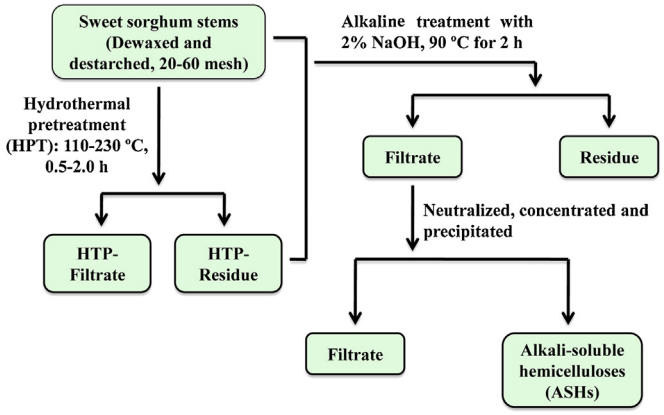

Fig. 1. Schematic diagram of the hemicelluloses extracted from the integrated process.

2.4. Analysis procedures

The neutral sugar, uronic acid compositions, and molecular weights of the ASHs were analyzed according to the procedure described in a previous paper (Sun, Wen, Ma, & Sun, 2013). The solution-state NMR spectra of the ASHs were acquired on a Bruker AVIII 400 MHz spectrometer at 25 °C. Soluble-state ^{1}H, ^{13}C, and HSQC NMR spectra were recorded according to the literature (Sun, Wen, Ma, & Sun, 2013). FT-IR spectra of the ASHs were recorded on a Bruker spectrophotometer in the range of 400–4000 cm^{-1} with a resolution of 4 cm^{-1}. KBr disk containing 1% finely ground sample was used for determination. Thermal stabilities of the ASHs were determined as described previously (Sun, Wen, Ma, & Sun, 2013).

3. Results and discussion

3.1. Yields and contents of neutral sugars

The contents of hemicelluloses in the HTP residues obtained from the different pretreatment conditions (110, 130, and 150 °C for 1.0 h, and 170 °C for 0.5) were 27.9, 27.4, 24.9, and 16.7% as determined by the NREL standard analytical procedure (Sluiter et al., 2011), respectively. The results indicated that the content of hemicelluloses was gradually decreased with the increasing pretreatment temperature, which was attributed to the autohydrolysis reaction of hemicelluloses during the HTP process. The yields of HR, $H_{110(1.0)}$, $H_{130(1.0)}$, $H_{150(1.0)}$, and $H_{170(0.5)}$ (based on the hemicelluloses in the HTP residue) are listed in Table 1. The increase of the pretreatment temperature from 110 to 130 °C resulted in an obvious increase of ASH yield from 54.9% to 60.6%. Nevertheless, when the pretreatment temperature was further increased to 170 °C, the ASH yield sharply decreased to 29.7%, implying that the drastic HTP process led to the significant degradation of hemicellulosic polymers, as revealed by the subsequent NMR spectra.

Table 1 shows the constituent sugar compositions of the ASHs. These ASHs contained mostly xylose and arabinose together with small amounts of galactose, glucose, glucuronic acid and galacturonic acid. The subsequent NMR data confirmed the presence of small amounts of glucuronic acid and indicated that they were arabinoglucuronoxylans (Maes & Delcour, 2001). The ratio of xylose to arabinose (Xyl/Ara) is indicative of the degree of linearity or

Table 1
Yield and contents of neutral sugars and uronic acids (relative %, w/w) of the hemicellulosic fractions (HR, $H_{110(1.0)}$, $H_{130(1.0)}$, $H_{150(1.0)}$, and $H_{170(0.5)}$) obtained from the integrated process.

	Ara[b]	Gal	Glu	Xyl	GlcA	GalA	Xyl/Ara[c]	Yield[d]
HR[a]	17.5	2.7	4.1	75.1	0.5	0.1	4.3	55.8
$H_{110(1.0)}$	18.8	2.5	3.1	74.7	0.6	0.3	4.0	54.9
$H_{130(1.0)}$	16.4	2.0	2.4	78.6	0.4	0.2	4.8	60.6
$H_{150(1.0)}$	15.3	2.4	2.8	79.1	0.3	0.1	5.2	30.9
$H_{170(0.5)}$	8.0	2.5	3.9	85.6	ND[e]	ND	10.7	29.7

[a] $H_{110(1.0)}$, $H_{130(1.0)}$, $H_{150(1.0)}$, and $H_{170(0.5)}$ represent the hemicellulosic fractions isolated by extraction with 2% NaOH aqueous solution at 90 °C for 2 h corresponding to the hydrothermal pretreatment temperature/time at 110 °C/1.0 h, 130 °C/1.0 h, 150 °C/1.0 h, and 170 °C/0.5 h, respectively. HR was also fractionated from the unpretreated material under the same alkaline treatment condition.
[b] Abbreviations: Ara, arabinose; Gal, galactose; Glc, glucose; Xyl, xylose; GlcA, glucuronic acid; GalA, galacturonic acid.
[c] Represent xylose to arabinose ratio.
[d] Based on the hemicelluloses in the corresponding HTP residue (%, w/w).
[e] ND, not detectable.

branching of hemicellulosic polymers (Wedig, Jaster, & Moore, 1987). In this study, the Xyl/Ara of the ASHs increased with the increasing pretreatment temperature from 110 to 170 °C, suggesting that the ASHs extracted at the higher pretreatment temperatures had a more linear structure (Table 1) (Sun, Lawther, & Banks, 1996). This fact also suggested that most of the side chains in hemicelluloses were significantly cleaved under the harsh conditions (≥170 °C).

3.2. Molecular weight analysis

Table 2 exhibits weight-average (M_w) and number-average (M_n) molecular weights along with polydispersity indexes (PDIs, M_w/M_n) of the ASHs. Evidently, HR (not hydrothermally pretreated) showed the highest molecular weight and molecular weight decreased with increasing pretreatment temperature. This fact indicated that the HTP process resulted in the lower molecular weight in the four hydrothermally pretreated hemicelluloses ($H_{110(1.0)}$, $H_{130(1.0)}$, $H_{150(1.0)}$, and $H_{170(0.5)}$). Generally, the degree of hemicelluloses hydrolysis increase as the HTP severity increase. The reason for this is that the hydronium ions release by the water during the HTP and result in depolymerization of hemicelluloses by selective hydrolysis of glycosidic linkages, liberating O-acetyl group and other acid moieties to form acetic and uronic acids. The release of these acids during the HTP is thought to catalyze the hydrolysis of hemicelluloses and oligosaccharides, especially at the higher temperatures (Pu, Hu, Huang, Davison, & Ragauskas, 2013). As expected, in this study, an increment of the pretreatment temperature from 110 to 170 °C resulted in a gradual decrease of M_w from 63,650 to 11,100 g/mol, suggesting that the C–O bonds of ASHs were gradually cleaved, especially at the higher temperatures (≥170 °C). In addition, these ASHs with lower PDIs (1.19–2.16) implied that the HTP process yielded more homogeneous hemicellulosic polymers.

Table 2
Weight-average (M_w) and number-average (M_n) molecular weights and polydispersity (M_w/M_n) of the hemicellulosic fractions (HR, $H_{110(1.0)}$, $H_{130(1.0)}$, $H_{150(1.0)}$, $H_{170(0.5)}$) obtained from the integrated process.

	Hemicellulosic fractions[a]				
	HR	$H_{110(1.0)}$	$H_{130(1.0)}$	$H_{150(1.0)}$	$H_{170(0.5)}$
M_w	64,260	63,650	49,310	16,960	11,100
M_n	29,580	29,470	25,280	12,990	9290
M_w/M_n	2.17	2.16	1.95	1.31	1.19

[a] Corresponding to the hemicellulosic fractions in Table 1.

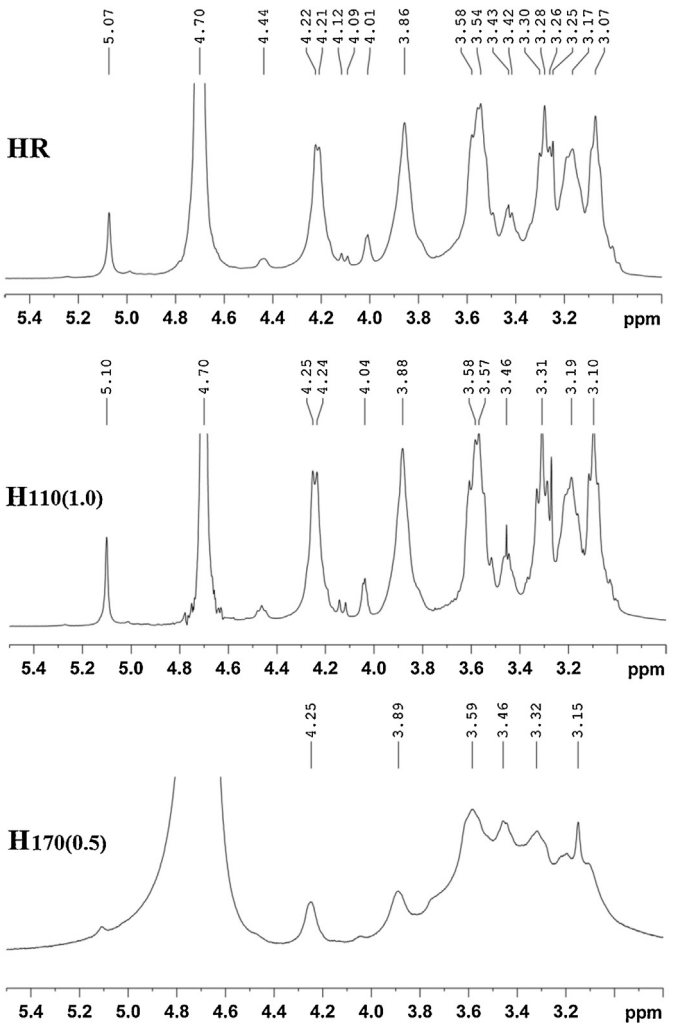

Fig. 2. ^{1}H NMR spectra of the hemicelluloses (HR, $H_{110(1.0)}$, and $H_{170(0.5)}$) obtained from the integrated process.

3.3. NMR spectral analysis

In this study, NMR spectroscopy was used to investigate the polymer backbone and the types of side-chain branching along the backbone of the ASHs. Fig. 2 (^{1}H NMR), Fig. 3 (^{13}C NMR), and Fig. 4 (2D-HSQC) exhibited the structural information of the ASHs (HR, $H_{110(1.0)}$, and $H_{170(0.5)}$) and the signals were assigned according to the previous literature (Billa, Koullas, Monties, & Koukios, 1997; Sun, Wen, Ma, & Sun, 2013; Sun et al., 2014; Teleman, Lundqvist, Tjerneld, Stålbrand, & Dahlman, 2000). As can be seen from the ^{1}H NMR spectra of HR and $H_{110(1.0)}$ (Fig. 2), the main signals at 4.22 (H-1), 3.86 (H-5eq), 3.54 (H-4), 3.28 (H-3), 3.17 (H-5ax), and 3.07 (H-2) ppm are assigned to β-D-xylopyranosyl (β-D-Xyl*p*) units, while a minor signal of anomeric protons of terminal arabinofuranosyl units was observed at 5.07 ppm, which was overlapped with that of 4-*O*-Me-α-D-Glc*p*A units. The ^{13}C NMR spectra of HR and $H_{110(1.0)}$ (Fig. 3) showed five strong signals at 102.2, 76.0, 74.8, 73.2, and 63.3 ppm, which are assigned to C-1, C-4, C-3, C-2, and C-5 of β-D-Xylp units. Other weaker signals at 109.5, 86.4, 78.4, 80.3, and 61.7 ppm, corresponding to C-1, C-4, C-3, C-2, and C-5 of α-L-arabinofuranosyl units, were also detected. Meanwhile, a small characteristic signal at 59.6 ($-OCH_3$) ppm, originating from 4-*O*-Me-α-D-Glc*p*A units, was observed in the spectra of HR and $H_{110(1.0)}$ but sharply decreased in $H_{170(0.5)}$, suggesting that the 4-*O*-Me-α-D-Glc*p*A units was degraded during the harsh pretreatment

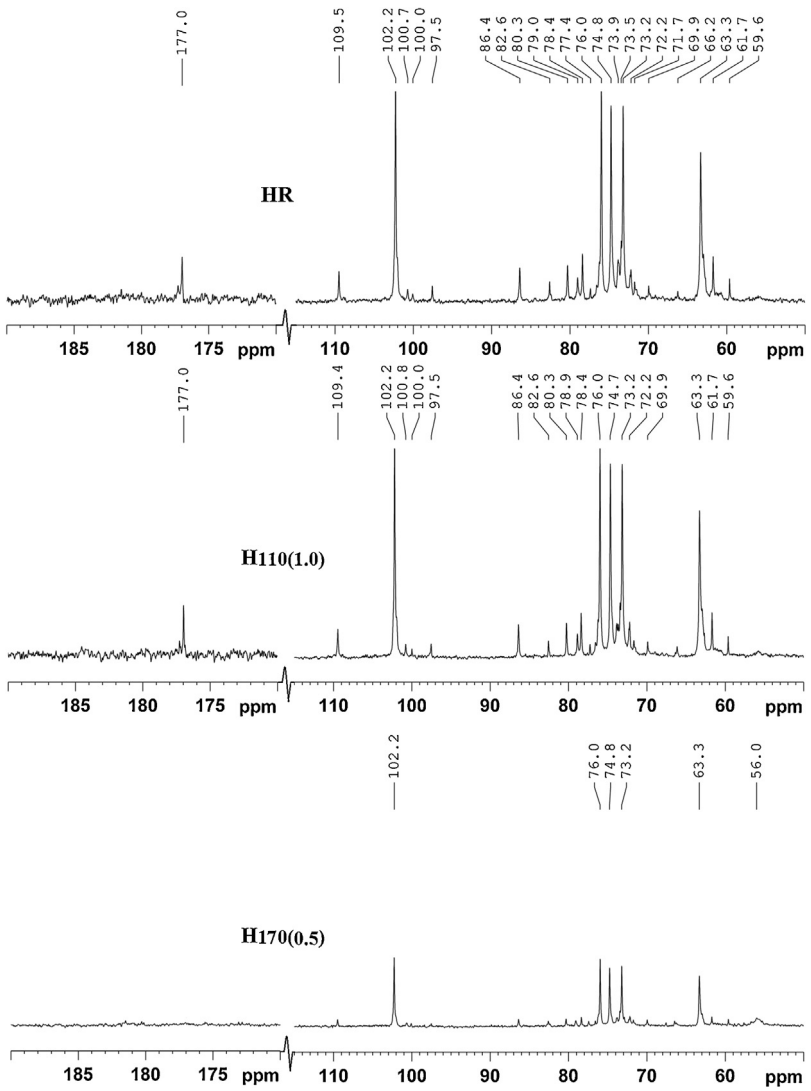

Fig. 3. ^{13}C NMR spectra of the hemicelluloses (HR, $H_{110(1.0)}$, and $H_{170(0.5)}$) obtained from the integrated process.

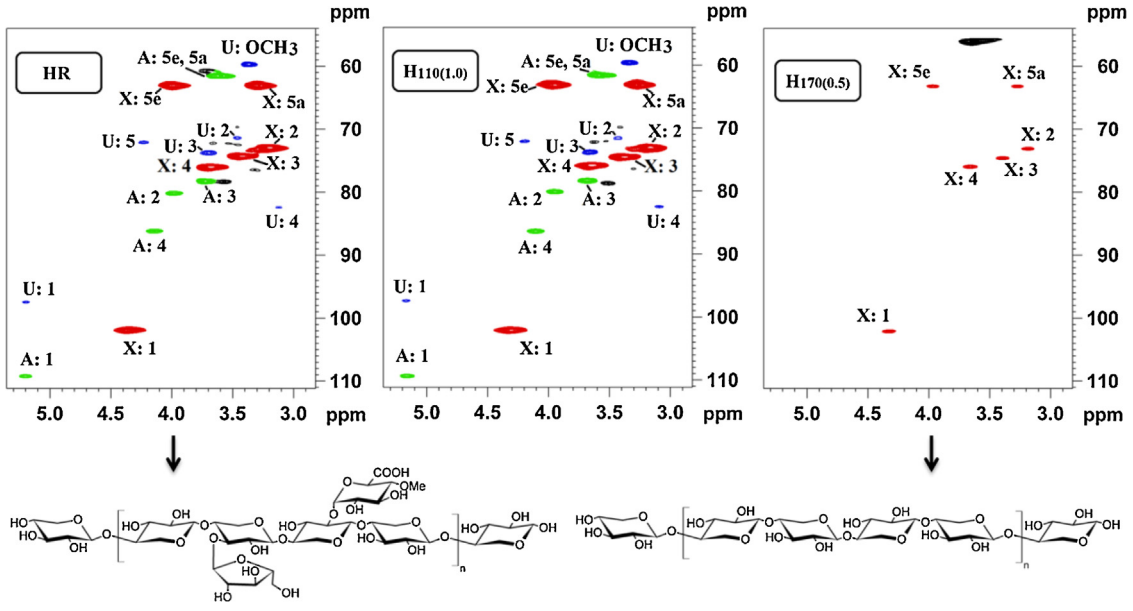

Fig. 4. 2D HSQC NMR spectral and the proposed structure of the hemicelluloses (HR, $H_{110(1.0)}$, and $H_{170(0.5)}$) obtained from the integrated process.

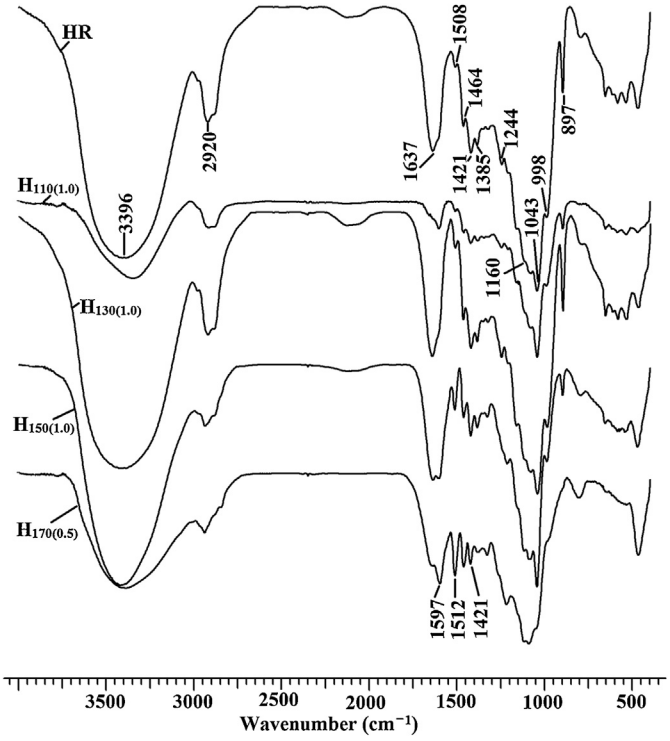

Fig. 5. FT-IR spectra of the hemicelluloses (HR, $H_{110(1.0)}$, $H_{130(1.0)}$, $H_{150(1.0)}$, and $H_{170(0.5)}$) obtained from the integrated process.

conditions. It was noted that only the signals of β-D-Xyl*p* units were shown in the ^{13}C NMR spectrum of $H_{170(0.5)}$ as compared with HR and $H_{110(1.0)}$, indicating a significant degradation of the hemicellulosic branches during the pretreatment at 170 °C for 0.5 h.

To further reveal structural features of the ASHs obtained from the integrated process, the more detailed structural information of HR, $H_{110(1.0)}$, and $H_{170(0.5)}$ were investigated by 2D-HSQC NMR spectra (Fig. 4). For HR and $H_{110(1.0)}$, five major cross-signals at 102.2/4.35, 73.2/3.19, 74.8/3.42, 76.0/3.68, 63.3/3.99, and 63.3/3.28 ppm, corresponding to the C_1–H_1, C_2–H_2, C_3–H_3, C_4–H_4, C_{5eq}–H_{5eq}, and C_{5ax}–H_{5ax} of (1 → 4)-linked β-D-Xyl*p* units, respectively, were clearly identified. Furthermore, the signals of α-L-arabinofuranosyl units were observed at 109.5/5.20, 80.3/3.98, 78.4/3.72, 86.4/4.14, and 61.7/3.59 ppm, which are characteristic of C_1–H_1, C_2–H_2, C_3–H_3, C_4–H_4, and C_5–H_5, respectively. Simultaneously, some weak cross-peaks at 97.5/5.20, 71.2/3.46, 73.8/3.70, 82.4/3.12, 72.1/4.23, and 59.6/3.36 ppm are originated from C_1–H_1, C_2–H_2, C_3–H_3, C_4–H_4, C_5–H_5, and –OCH_3 of 4-*O*-Me-α-D-Glc*p*A units in the HSQC spectra of HR and $H_{110(1.0)}$, respectively (Sun, Li, Yuan, Xu, & Sun, 2012). However, when the pretreatment temperature was further increased to 170 °C and kept for 0.5 h, only the cross-signals of β-D-Xyl*p* units were found in the HSQC spectrum of $H_{170(0.5)}$, implying that the glucosidic bonds in the hemicellulosic macromolecules were significantly cleaved when the HTP temperature reached 170 °C, which resulted in the $H_{170(0.5)}$ had the xylan-rich hemicellulosic polymers. This was also in accordance with the results of ^1H and ^{13}C NMR spectra. These results suggested that the degradation degree of hemicelluloses increased with the pretreatment temperature increased, as revealed by the aforementioned the molecular weight analysis.

3.4. FT-IR spectral analysis

The FT-IR spectra of the ASHs (HR, $H_{110(1.0)}$, and $H_{130(1.0)}$, $H_{150(1.0)}$, and $H_{170(0.5)}$) are illustrated in Fig. 5. As can be seen, the HR, $H_{110(1.0)}$, and $H_{130(1.0)}$ exhibited similar spectroscopic patterns, implying the similar structures of the ASHs. An intense band at 3396 cm^{-1} is originated from the –OH stretching vibrations and the band at 2920 cm^{-1} corresponds to the C–H stretching of the ASHs. An intensive band at 1633 cm^{-1} was mainly associated with absorbed water as a result of a strong affinity of water to hemicelluloses. In the solid state these macromolecules may have disordered structures, which could easily be hydrated (Kačuráková, Belton, Wilson, Hirsch, & Ebringerová, 1998). The rather weaker bands at 1508 and 1421 cm^{-1} in the ASHs are originated from the aromatic skeletal vibrations in associated lignin. The bands at 1464 and 1385 cm^{-1} are assigned to $-CH_2$ stretching and CH or OH bending, respectively. The absorption band at 1244 cm^{-1} is attributed to the C–O linkage in the acetyl group of hemicelluloses (Bastawde, 1992). The weak bands at 1160 and 998 cm^{-1} are indication of arabinosyl side chains, which have been reported to be attached only at position C-3 of xylopyranosyl constituents (Kacurakova, Capek, Sasinkova, Wellner, & Ebringerova, 2000). The results suggested that the β-(1 → 4)-xylan was linked with a small amount of arabinose, as confirmed by sugar analysis of the ASHs (Sun & Tomkinson, 2002). The band at 1043 cm^{-1} is due to the C–O–C stretching of glycosidic linkages, which is representative of xylans in the ASHs (Kačuráková, Ebringerova, Hirsch, & Hromadkova, 1994). In addition, a sharp band at 897 cm^{-1} is indicative of β-(1 → 4)-glycosidic bond between the xylose units in the ASHs (Gupta, Madan, & Bansal, 1987; Kacurakova et al., 2000). Based on the results of sugar analyses, NMR, and FT-IR, the structure of HR and $H_{110(1.0)}$ was assumed to be L-arabino-4-*O*-methyl-D-glucurono-D-xylan (Habibi, Mahrouz, & Vignon, 2002; Sun, Wen, Ma, & Sun, 2013). However, some typical characteristic bands (i.e., 1597, 1512, and 1421 cm^{-1}) of lignin were observed in the spectra of $H_{150(1.0)}$ and $H_{170(0.5)}$, suggesting that part of lignin was released and co-precipitated or still linked with hemicelluloses in these ASHs when the pretreatment temperature exceeded 130 °C (Sun, Wen, Ma, Li, & Sun, 2013).

3.5. Thermal analysis

The thermal properties of HR, $H_{110(1.0)}$ and $H_{170(0.5)}$ were investigated (Fig. 6) by TGA and differential thermogravimetry (DTG). The three hemicellulosic fractions were found to be initially decomposed at about 200 °C, and their maximum decomposition temperature (T_{max}) was observed from 250 to 320 °C (the main decomposition stage) (Hodgson et al., 2011). Specifically, the T_{max} of HR, $H_{110(1.0)}$, and $H_{170(0.5)}$ were 294.19, 299.27, and 292.21 °C, respectively. In the main stage, the thermal decomposition process can be resulting from the cracking and abscission of C–O bonds connected with the main chains of xylan in the ASHs. In addition, decarboxylation and decarbonylation may also occur, thus resulting in high pyrogenic decomposition reactivity in ASHs. Eventually, the ASHs decomposed into CO, CO_2, and some light hydrocarbon (such as CH_4 and C_2H_4) (Yang, Yan, Chen, Lee, & Zheng, 2007). Notably, when the temperature surpassed 350 °C, the weight loss of the ASHs was very slight, and devolatilization occurred until the temperature reached 700 °C. It was found that the contents of "solid residues (SR)" at 700 °C were 35% for HR and 16% for $H_{110(1.0)}$, respectively. The fact was probably related to the HTP process, which partly removed ash and inorganic salt from SSS, whereas most of ash and inorganic salt were remained in the unpretreated SSS (Kirubakaran et al., 2009). In addition, the content of SR at 700 °C reached 54% in $H_{170(0.5)}$, which was probably attribute to some co-precipitated and condensed lignin in $H_{170(0.5)}$ (Wen, Sun, Xue, & Sun, 2013).

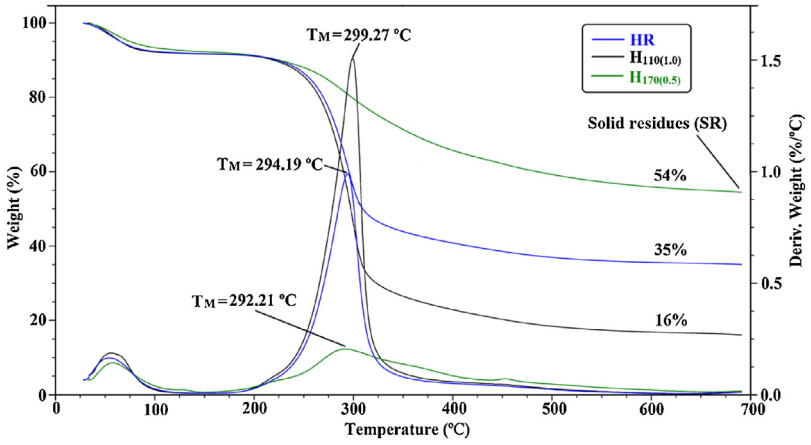

Fig. 6. TG/DTG curves of spectra of the hemicelluloses (HR, $H_{110(1.0)}$, and $H_{170(0.5)}$) obtained from the integrated process.

4. Conclusions

In this study, an integrated process based on multiple HTP and alkaline treatment was used to obtain hemicelluloses from SSS. The isolated ASH with the highest yield (60.6%) was obtained from the HTP residue performed at 130 °C for 1.0 h. The isolated hemicellulosic polymers had a more linear structure with an increase of the pretreatment temperature from 110 to 170 °C. The M_w and M_n of the ASHs decreased as the pretreatment temperature increased, implying that the C–O bonds of the ASHs was significantly cleaved, especially at the harsh conditions (≥170 °C). In addition, these ASHs with lower PDIs (1.19–2.16) indicated that the HTP combined alkaline processes yielded more homogeneous hemicellulosic polymers as compared to HR (PDI, 2.17) obtained from the unpretreated material. The structure of the ASHs obtained from the integrated process was assumed to be L-arabino-4-*O*-methyl-D-glucurono-D-xylan.

Acknowledgements

The authors are extremely grateful to financial support from the 10-25 project (2012BAD32B06) and Major State Basic Research Projects of China (973-2010CB732203).

References

Alfani, F., Gallifuoco, A., Saporosi, A., Spera, A., & Cantarella, M. (2000). Comparison of SHF and SSF processes for the bioconversion of steam-exploded wheat straw. *Journal of Industrial Microbiology and Biotechnology*, *25*(4), 184–192.

Antonopoulou, G., Gavala, H. N., Skiadas, I. V., Angelopoulos, K., & Lyberatos, G. (2008). Biofuels generation from sweet sorghum: fermentative hydrogen production and anaerobic digestion of the remaining biomass. *Bioresource Technology*, *99*(1), 110–119.

Balat, M., Balat, H., & Öz, C. (2008). Progress in bioethanol processing. *Progress in Energy and Combustion Science*, *34*(5), 551–573.

Bastawde, K. (1992). Xylan structure, microbial xylanases, and their mode of action. *World Journal of Microbiology and Biotechnology*, *8*(4), 353–368.

Berndes, G., Hoogwijk, M., & van den Broek, R. (2003). The contribution of biomass in the future global energy supply: A review of 17 studies. *Biomass and Bioenergy*, *25*(1), 1–28.

Billa, E., Koullas, D. P., Monties, B., & Koukios, E. G. (1997). Structure and composition of sweet sorghum stalk components. *Industrial Crops and Products*, *6*(3), 297–302.

Gabrielii, I., Gatenholm, P., Glasser, W., Jain, R., & Kenne, L. (2000). Separation, characterization and hydrogel-formation of hemicellulose from aspen wood. *Carbohydrate Polymers*, *43*(4), 367–374.

Garrote, G., Dominguez, H., & Parajó, J. C. (1999). Mild autohydrolysis: an environmentally friendly technology for xylooligosaccharide production from wood. *Journal of Chemical Technology and Biotechnology*, *74*(11), 1101–1109.

Gupta, S., Madan, R., & Bansal, M. (1987). Chemical composition of Pinus caribaea hemicellulose. *Tappi Journal*, *70*, 113–114.

Habibi, Y., Mahrouz, M., & Vignon, M. R. (2002). Isolation and structure of D-xylans from pericarp seeds of *Opuntia ficus-indica* prickly pear fruits. *Carbohydrate Research*, *337*(17), 1593–1598.

Hodgson, E., Nowakowski, D., Shield, I., Riche, A., Bridgwater, A. V., Clifton-Brown, J. C., et al. (2011). Variation in *Miscanthus* chemical composition and implications for conversion by pyrolysis and thermo-chemical bio-refining for fuels and chemicals. *Bioresource Technology*, *102*(3), 3411–3418.

Jørgensen, H., Kristensen, J. B., & Felby, C. (2007). Enzymatic conversion of lignocellulose into fermentable sugars: Challenges and opportunities. *Biofuels, Bioproducts and Biorefining*, *1*(2), 119–134.

Kabel, M., Carvalheiro, F., Garrote, G., Avgerinos, E., Koukios, E., Parajó, J., et al. (2002). Hydrothermally treated xylan rich by-products yield different classes of xylo-oligosaccharides. *Carbohydrate Polymers*, *50*(1), 47–56.

Kačuráková, M., Belton, P. S., Wilson, R. H., Hirsch, J., & Ebringerová, A. (1998). Hydration properties of xylan-type structures: An FTIR study of xylooligosaccharides. *Journal of the Science of Food and Agriculture*, *77*(1), 38–44.

Kačuráková, M., Ebringerova, A., Hirsch, J., & Hromadkova, Z. (1994). Infrared study of arabinoxylans. *Journal of the Science of Food and Agriculture*, *66*(3), 423–427.

Kacurakova, M., Capek, P., Sasinkova, V., Wellner, N., & Ebringerova, A. (2000). FT-IR study of plant cell wall model compounds: Pectic polysaccharides and hemicelluloses. *Carbohydrate Polymers*, *43*(2), 195–203.

Kirubakaran, V., Sivaramakrishnan, V., Nalini, R., Sekar, T., Premalatha, M., & Subramanian, P. (2009). A review on gasification of biomass. *Renewable and Sustainable Energy Reviews*, *13*(1), 179–186.

Leu, S. Y., & Zhu, J. (2012). Substrate-related factors affecting enzymatic saccharification of lignocelluloses: our recent understanding. *BioEnergy Research*, *6*(2), 405–415.

Liu, S. (2010). Woody biomass: Niche position as a source of sustainable renewable chemicals and energy and kinetics of hot-water extraction/hydrolysis. *Biotechnology Advances*, *28*(5), 563–582.

Lloyd, T. A., & Wyman, C. E. (2005). Combined sugar yields for dilute sulfuric acid pretreatment of corn stover followed by enzymatic hydrolysis of the remaining solids. *Bioresource Technology*, *96*(18), 1967–1977.

Maes, C., & Delcour, J. (2001). Alkaline hydrogen peroxide extraction of wheat bran non-starch polysaccharides. *Journal of Cereal Science*, *34*(1), 29–35.

Prasad, S., Singh, A., Jain, N., & Joshi, H. (2007). Ethanol production from sweet sorghum syrup for utilization as automotive fuel in India. *Energy & Fuels*, *21*(4), 2415–2420.

Pu, Y. Q., Hu, F., Huang, F., Davison, B. H., & Ragauskas, A. J. (2013). Assessing the molecular structure basis for biomass recalcitrance during dilute acid and hydrothermal pretreatments. *Biotechnology for Biofuels*, *6*(1), 15.

Reddy, B. V., Ramesh, S., Reddy, P. S., Ramaiah, B., Salimath, M., & Kachapur, R. (2005). Sweet sorghum – A potential alternate raw material for bio-ethanol and bio-energy. *International Sorghum and Millets Newsletter*, *46*, 79–86.

Sluiter, A., Hames, B., Ruiz, R., Scarlata, C., Sluiter, J., Templeton, D., & Crocker, D. (2011). Determination of structural carbohydrates and lignin in biomass. *Laboratory Analytical Procedure*,. http://www.nrel.gov/biomass/analytical_procedures.html

Sun, R. C. (2009). Detoxification and separation of lignocellulosic biomass prior to fermentation for bioethanol production by removal of lignin and hemicelluloses. *BioResources*, *4*(2), 452–455.

Sun, R. C., Lawther, J. M., & Banks, W. (1996). Fractional and structural characterization of wheat straw hemicelluloses. *Carbohydrate Polymers*, *29*(4), 325–331.

Sun, R. C., & Tomkinson, J. (2002). Characterization of hemicelluloses obtained by classical and ultrasonically assisted extractions from wheat straw. *Carbohydrate Polymers*, *50*(3), 263–271.

Sun, S. L., Wen, J. L., Ma, M. G., Li, M. F., & Sun, R. C. (2013). Revealing the structural inhomogeneity of lignins from sweet sorghum stem by successive alkali extractions. *Journal of Agricultural and Food Chemistry*, *61*(18), 4226–4235.

Sun, S. L., Wen, J. L., Ma, M. G., & Sun, R. C. (2013). Successive alkali extraction and structural characterization of hemicelluloses from sweet sorghum stem. *Carbohydrate Polymers*, *92*(2), 2224–2231.

Sun, S. N., Cao, X. F., Xu, F., Sun, R. C., Jones, G. L., & Baird, M. (2014). Structure and thermal property of alkaline hemicelluloses from steam exploded *Phyllostachys pubescens*. *Carbohydrate Polymers*, *101*, 1191–1197.

Sun, S. N., Li, M. F., Yuan, T. Q., Xu, F., & Sun, R. C. (2012). Effect of ionic liquid pretreatment on the structure of hemicelluloses from corncob. *Journal of Agricultural and Food Chemistry*, *60*(44), 11120–11127.

Sun, Y., & Cheng, J. (2002). Hydrolysis of lignocellulosic materials for ethanol production: A review. *Bioresource Technology*, *83*(1), 1–11.

Teleman, A., Lundqvist, J., Tjerneld, F., Stålbrand, H., & Dahlman, O. (2000). Characterization of acetylated 4-*O*-methylglucuronoxylan isolated from aspen employing ^{1}H and ^{13}C NMR spectroscopy. *Carbohydrate Research*, *329*(4), 807–815.

Thomsen, M. H., Thygesen, A., & Thomsen, A. B. (2008). Hydrothermal treatment of wheat straw at pilot plant scale using a three-step reactor system aiming at high hemicellulose recovery, high cellulose digestibility and low lignin hydrolysis. *Bioresource Technology*, *99*(10), 4221–4228.

Wedig, C. L., Jaster, E. H., & Moore, K. J. (1987). Hemicellulose monosaccharide composition and in vitro disappearance of orchard grass and alfalfa hay. *Journal of Agricultural and Food Chemistry*, *35*(2), 214–218.

Wen, J. L., Sun, S. L., Xue, B. L., & Sun, R. C. (2013). Quantitative structures and thermal properties of birch lignins after ionic liquid pretreatment. *Journal of Agricultural and Food Chemistry*, *61*(3), 635–645.

Yang, H., Yan, R., Chen, H., Lee, D. H., & Zheng, C. (2007). Characteristics of hemicellulose, cellulose and lignin pyrolysis. *Fuel*, *86*(12), 1781–1788.

Zhang, H., & Wu, S. (2013). Subcritical CO_2 pretreatment of sugarcane bagasse and its enzymatic hydrolysis for sugar production. *Bioresource Technology*, *149*, 546–550.

Zhao, Y. L., Dolat, A., Steinberger, Y., Wang, X., Osman, A., & Xie, G. H. (2009). Biomass yield and changes in chemical composition of sweet sorghum cultivars grown for biofuel. *Field Crops Research*, *111*(1), 55–64.